Title
IN SITU OBSERVATIONS OF THE NITRIDING OF TANTALUM

Permalink
https://escholarship.org/uc/item/4812z4qq

Authors
Swann, P.R.
Thomas, G.
Tighe, N.J.

Publication Date
1972-12-01

To be Published in Journal
of Microscopy

LBL-1196
Preprint C1

IN SITU OBSERVATIONS OF THE NITRIDING OF TANTALUM

P. R. Swann, G. Thomas and N. J. Tighe

December 1972

Prepared for the U. S. Atomic Energy Commission
under Contract W-7405-ENG-48

In situ observations of the nitriding of tantalum

by P. R. SWANN, G. THOMAS* *and* N. J. TIGHE, *Department of Metallurgy, Imperial College, London SW7 2BP, and *Department of Materials, Science and Engineering, Berkeley, California* 94720

SUMMARY

A gas reaction cell developed for the AEI EM7 has been used to observe directly the structural changes which occur when tantalum is heated in nitrogen. It is demonstrated that sharp images of the microstructure can be obtained from specimens at temperature while surrounded by a 5·5 mm thick layer of the reaction gas at a pressure of 35 torr. The usefulness of the *in situ* technique for studying gas/metal reactions is assessed.

INTRODUCTION

In the past 10 years electron microscopy and diffraction have provided considerable evidence for ordering in dilute solutions of interstitials (~ 1 at %) in group Va bcc metals, e.g. carbon (Villagrana & Thomas, 1965), oxygen (van Torne & Thomas, 1964); van Landuyt, Gevers & Amelinckx, 1966), nitrogen (Seraphin, Stemple & Novick, 1962), but the mechanisms of the ordering transitions are not fully understood. The reactions are important since they appear to be associated with the well known ductile/brittle transition that occurs in refractory metals. Other points of interest stem from the fact that the crystal structures of the ordered phases are different for various members of the group and elasticity arguments (Beshers, 1965) have been used which suggest that this is due to a transition from octahedral to tetrahedral occupancy of the interstitials in the different bcc metals.

In this paper we describe some preliminary observations of the structural changes which occur during the nitriding of tantalum in a special environmental cell mounted in the AEI EM7 (Swann & Tighe, 1971). The advantages of carrying out the nitriding reaction *in situ* are (1) the changes in structure of a particular region of a specimen can be followed throughout the reaction (2) the experimental conditions required to produce the structure of interest can be obtained very quickly by visual observation (3) effects occurring at temperature in the environment can be readily distinguished from those which occur on cooling from the reaction temperature. The disadvantage of the *in situ* technique are (1) thin film effects may lead to structures which are not typical of the bulk (2) the composition of the specimen is non-uniform because of variations in thickness and surface reactivity (3) specimen contamination and electron irradiation may locally influence the reaction kinetics and products (4) the temperature of the specimen is difficult to determine accurately since the pressure of the gaseous environment affects the temperature difference between the specimen and the heater and also the power required to achieve a certain heater temperature.

EXPERIMENTAL PROCEDURE

Cold rolled tantalum sheet 99·9% purity was recrystallized by resistance heating to 1200°C in a pressure of 5×10^{-7} torr ($6{\cdot}67 \times 10^{-5}$ N/m²). The specimens were prepared for electron microscopy by electropolishing in a solution containing one part sulphuric acid and seven parts methanol at 12 V and −30°C. Specimens were washed and dried as quickly as possible before placing in a ribbon heater hot stage specially developed for the environmental cell of the AEI EM7 (Swann, 1972).

Separate experiments were carried out to determine the difference between the heater temperature and the specimen temperature at various gas pressures. For these experiments 100 μm diameter thermocouple wires were spot welded to a

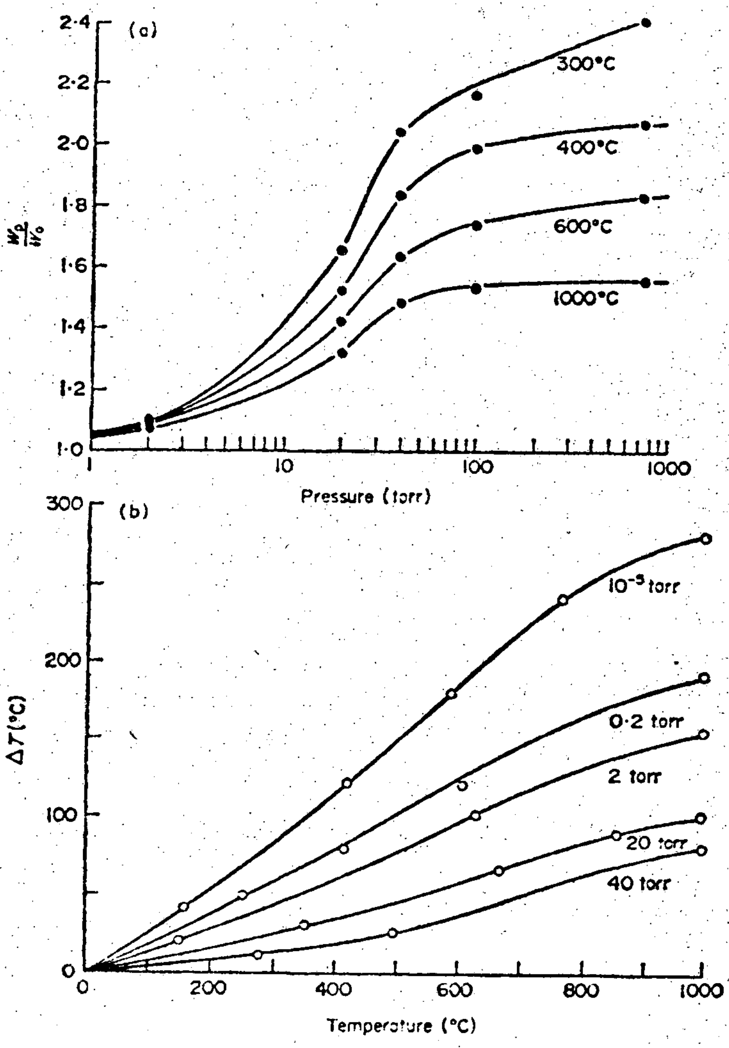

Fig. 1. (a) Temperature difference between a specimen and a supporting strip heater versus heater temperature and air pressure. (b) Pressure dependence of the heater power required to achieve the indicated temperatures, W_p, relative to the power required at 10^{-5} torr, W_0.

disc specimen and also adjacent to the specimen on the underside of the heater. The specimen was heated by alternating current to eliminate pick-up errors in the thermocouple readings.

RESULTS

The temperature difference, ΔT, between the heater and the specimen is shown in Fig. 1a for various gas pressures in the range 10^{-5} torr (1·33 mN/m^2) to 60 torr (8 kN/m^2). The power required to achieve a cetain heater temperature was also measured as a function of a gas pressure. The results, normalized with respect to the power required at 10^{-5} torr (1·33 mN/m^2) are shown in Fig. 1b.

The above results were used to estimate the temperature of the tantalum specimen in relation to the heater temperature during the nitriding experiments. It was found that the reaction proceeded at a convenient rate with good specimen visibility at a nitrogen pressure of 35 torr (4·67 kN/m^2) and an estimated specimen temperature of 300°C ± 10°C. The first visible evidence of the nitriding reaction occurred at the thin edges of the electron microscope specimen. The product takes the form of a fine tweed-like structure which is shown in Fig. 2. Detailed examination of the micrographs reveals that the fine striations which form the tweed-like structure are thin plates parallel to $\{110\}$ of the bcc tantalum lattice. A typical diffraction pattern of the tweed structure is shown in Fig. 3a and compared with a diffraction pattern of the same area before nitriding in Fig. 3b. The analysis of diffraction patterns in the nitriding materials is complicated by the existence of several variants of the structure lying in the area covered by the diffraction aperture and also by the occurrence of multiple diffraction. However, it was found that isolated variants of the reaction product would occasionally form in specimens coated with a protective film produced by contamination in the electron beam or by exposure to the atmosphere for a long time before nitriding. A diffraction pattern from a single variant in the bcc matrix is shown in Fig. 4a. Comparison with Fig. 3b shows that the bright reflections correspond to the fundamental reflections of the bcc tantalum structure and since the extra reflections in the nitrided structure occur at perfect fractions of the bcc interplanar spacing they most likely arise from interstitial ordering of nitrogen atoms in the bcc structure. The pattern is analysed on this basis in Fig. 4b which is consistent with a superlattice with axes given approximately by $|a_1| = 2a$, $|a_2| = 4a$, $|a_3| = 4c$ where a is the lattice parameter of the original bcc structure and c is slightly longer than a as a consequence of the tetragonal distortion from the interstitial nitrogen. The c/a ratio calculated from the positions of reflections in Fig. 4b is 1·06 but this ratio varies from specimen to specimen which suggests that the superlattice can accommodate deviations from stoichiometry.

Continued heating of specimens in the nitrogen environment results in the appearance of a new structure with a lenticular morphology. The lenticular plates appear first at the thin edge of the electron microscope specimen. They are homogeneously distributed and repeatedly subdivide to merge with the tweed-like structure as the thickness of the specimen increases. A typical example of this morphology appears in Fig. 5. The plates themselves possess a fine internal substructure which is similar in appearance to the tweed structure.

With a further increase in nitrogen content, martensite-like plates propagate rapidly through the tweed structure into the thick parts of the specimen. The specimen movement resulting from this transformation prevented photographic recording and in order to obtain micrographs the specimen temperature was lowered by about 40°C to stop the transformation. An example of the martensitic structure is shown in Fig. 6. Eventually this structure completely fills the specimen and although several variants occur in any one grain it was observed (as in Fig. 7) that alternate plates often have similar orientations. This is clearly an example of co-operative growth frequently observed in martensite transformations and also seen by Potter & Altstetter (1972) in bulk specimens of nitrided vanadium. A consistent solution to the diffraction data of the martensitic product has not yet been obtained owing to the complexities introduced by streaking of diffraction maxima between reciprocal lattice layers, the appearance of several twinning variants inside a single plate and the inevitable appearance of more than one martensite variant in any one diffractional pattern. The patterns cannot be indexed in terms of the hexagonal vanadium nitride observed by Potter & Altstetter (1972). Attempts to analyse diffraction patterns have therefore been postponed until a method of coarsening the martensitic structure has been developed.

During the course of the experiments it was noticed that areas of the specimen examined before nitriding would react more slowly with nitrogen during subsequent heating (see for example Fig. 8). The effect is not due to radiation damage in the tantalum because it is also observed in specimens examined well below the threshold voltage for such damage. In further experiments it was noted that the nitriding reaction is not hindered if pre-examination of the specimen is carried out in an oxygen environment at a pressure of 30 torr. It is known from the work of Heide (1958) that carbon contamination does not occur under these conditions and this strongly suggests that the effect shown in Fig. 8 is due to a build up of carbon on the specimen surface which subsequently prevents nitrogen entering the specimen.

DISCUSSION

The results in Fig. 1a show that increasing the gas pressure around the hot stage decreases the temperature difference, ΔT, between the specimen and the heater. The value of ΔT may be as high as 280°C at a pressure of 10^{-5} torr (1·33 mN/m^2) and a heater temperature of 1000°C, but this can easily be reduced to 60°C by increasing the pressure at the specimen to 60 torr (8 kN/m^2). The actual temperature difference in a typical electron microscope hot stage experiment may be greater or less than indicated in Fig. 1a depending on the method of specimen clamping and the radiation shielding. However, the present work does indicate that the accuracy of electron microscope hot stages could be improved by providing an inert gas around the specimen to assist the heat transfer from the furnace. Figure 1b shows that the power required to achieve a certain specimen temperature in the gas reaction cell increases most rapidly in the pressure range 10–50 torr (1·33–6·65 kN/m^2) and thus to avoid excessive heat dissipation into the microscope when working at high temperatures, a gas pressure less than about 10 torr (1·33 kN/m^2) should be used. Figure 1b also demonstrates that one should not decrease the reaction gas pressure in an attempt to control the speed of a gas/solid reaction. In fact, this action would result in an immediate increase in heater temperature thereby increasing the reaction rate.

In the present experiments the working temperature required was only about 300°C and it was found that thermal drift of the specimen was not a serious problem at a nitrogen pressure of 35 torr. Consequently this pressure was chosen since ΔT at 300°C was only about 10°C.

The fine, tweed-like structure which forms at the beginning of the nitriding reaction (see for example Fig. 2) is best interpreted as an array of zones belonging to different variants of the ordered structure which fit together in a way which minimizes the total strain energy. The diffraction pattern in Fig. 3a shows that the zones are twin related about $\{110\}$ planes of the parent bcc structure. The characteristic absences among the reflections from the nitrogen sublattice suggest a body-centred symmetry and if it is assumed that the basis of the sublattice is a single nitrogen atom the stoichiometric composition of the ordered structure would be $Ta_{64}N$. However, in Fig. 4a, and in other diffraction patterns it was noted that reflections of the type $(h + k + l) = 4(2n + l)$ are either very weak or absent. This indicates a more complicated basis than one nitrogen atom and suggests that the ordered structure has a higher nitrogen content than $Ta_{84}N$.

In the nitriding experiments the ordering reaction is homogeneously nulceated and typically the surface density of nuclei is in excess of $2 \times 10^7/mm^2$. The nucleation rate can be reduced by nitriding at much lower nitrogen pressures or, more effectively, by encouraging surface contamination. Both actions result in a slower rate of entry of nitrogen into the specimen and permit coarser structures to develop. Under these conditions a well defined two phase, ordered/disordered structure was observed at the beginning of tantalum nitriding. This structure is similar to that observed at low oxygen pressures by van Landuyt (1964) in niobium–oxygen alloys and both observations suggest that the interstitial ordering reactions are not higher order phase changes (Christin 1965). The existence of a tetragonal distortion in the ordered structure suggests that the nitrogen atoms are located in octahedral rather than tetrahedral sites (van Landuyt & Wayman, 1968).

Transformations with a martensitic morphology are well known in bulk oxidation and nitriding reactions involving group Va metals (Kofstad, 1961; van Landuyt & Wayman, 1968; Potter & Altstetter, 1972). It has been shown by van Landuyt & Wayman, (1968) that the martensite plates form only near the gas/metal interface and they suggest that the transformation occurs when the surface layer becomes sufficiently supersaturated with respect to the interstitial atom. The present work supports this suggestion since at the reaction temperature the martensite plates propagate rapidly into the thick regions of the tantalum once they have nucleated in the nitrogen-rich regions at the edge of the specimen. In Fig. 6 it can be clearly seen that the growth rate at the tip of a martensite plate is uniform across the section of the specimen. This suggests that the driving force for plate growth results from a pre-existing nitrogen supersaturation and not from the continual take-up of nitrogen where the plate intersects the specimen surfaces. Thus, the transformation differs from conventional martensite where the driving force needed during the nucleation event derives from a decrease in temperature. During nitriding, the temperature is constant and the driving force derives from the change in nitrogen content. Thus, if nitride products are to form martensitically it is necessary for the up-take of nitrogen to be sufficiently rapid that the transformation does not occur via the competing diffusional process. This consideration as well as the higher elastic constraints in the bulk probably account for absence of plate formation away from the gas/metal interface.

CONCLUSION

It has been shown above that a nitriding reaction can be observed as it occurs in the electron microscope. It is clear that a wide range of other gas/solid reactions could also be studied directly using the same technique. The main attraction of the method is its ability to reveal the structural changes which occur during a surface reaction under typical service conditions. Unfortunately, however, the technique at its present state of development is not very useful for studying the equilibrium structures of a material as a function of composition. This is because it is difficult to control accurately the partial pressures of the reacting gases in the confined regions of the environmental cell. For such experiments, it is better to conduct the reaction in a separate closed system with a metered amount of the reacting gas so that the composition of the electron microscope specimen is known and remains constant during time required for the structure to reach equilibrium.

ACKNOWLEDGMENTS

We are grateful to Mr A. E. Lloyd and Mr R. Porter for their skilful construction of the gas reaction cell and the hot stage used in this work. We are also grateful to Mr C. R. Mayo who obtained the data plotted in Fig. 1a and b. G. Thomas acknowledges the award of a Guggenheim Fellowship and N. J. Tighe acknowledges the support of the USAF under grant number AFOSR-72-2360. The high voltage microscope facility used at the Department of Metallurgy, Imperial College, is operated by a grant from the Science Research Council.

References

Beshers, D.N. (1965) An investigation of interstitial sites in the bcc lattice. *J. appl. Phys.* **36**, 290.

Christian, J.W. (1965) *The Theory of Transformations in Metals and Alloys*. Pergamon Press, London.

Heide, H.G. (1958) Electron microscopic observations of specimens under controlled gas pressure. *J. Cell Biol.* **13**, 147.

Kofstad, P. (1961) Oxidation of tantalum in the temperature range 500–700°C. *J. Inst. Metals*, **90**, 253.

van Landuyt, J. (1964) An electron microscopic investigation of phenomena associated with solid solution of oxygen in niobium. *Phys. Stat. Sol.* **6**, 957.

van Landuyt, J., Gevers, R. & Amelinckx, S. (1966) Ordering of interstitial impurities in niobium. *Phys. Stat. Sol.* **13**, 467.

van Landuyt, J. & Wayman, C.M. (1968) A study of oxide plate formation in tantalum. *Acta metall.* **16**, 803.

Potter, D.I. & Altstetter, C. (1972) Phase transformations in concentrated V–N solutions. *Acta metall.* **20**, 313.

Seraphin, D.P., Stemple, N.R. & Novick, D.T. (1962) Phase instability in dilute interstitial solid solutions of nitrogen in tantalum. *J. appl. Phys.* **33**, 136.

Swann, P.R. & Tighe, N.J. (1971) High voltage microscopy of gas oxide reactions. *Jernkont. Annlr.* **155**, 497.

Swann, P.R. (1972) Side entry single tilt specimen holder for heating and stress corrosion cracking of electron microscope specimens. *Proc. 5th Europ. Cong. Electron Microsc.* 330.

van Torne, L.I. & Thomas, G. (1964) Phase transformations in niobium involving interstitials. *Acta metall.* **12**, 601.

Villagrana, R.E. & Thomas, G. (1965) Interstitial ordering of carbon in tantalum. *Phys. Stat. Sol.* **9**, 499.

Figure Captions

Fig. 1. (a) Temperature difference between a specimen and a supporting strip heater versus heater temperature and air pressure.
(b) Pressure dependence of the heater power required to achieve the indicated temperatures, W_p, relative to the power required at 10^{-5} torr, W_o.

Fig. 2. Fine tweed-like structure formed at the initial stage of the reaction between tantalum and nitrogen at 300°C ± 10°C and 35 torr (4.67 kN/m^2) nitrogen. Operating voltage 1 MV. × 54,000.

Fig. 3. (a) Typical diffraction pattern from a 111 zone of tantalum after the formation of the tweed structure.
(b) Same diffraction zone before niriding. Operating voltage 1 MV.

Fig. 4. (a) Similar diffraction zone to Fig. 3a, but showing a single variant of the ordered structure.
(b) Analysis of Fig. 4a. Operating voltage 1 MV.

Fig. 5. Lenticular plates growing from the thin edge of a tantalum specimen. Note the subdivision of the plates where they merge into the tweed structure and the substructure within each plate. Micrograph taken at 300°C in 35 torr of nitrogen. Operating voltage 1 MV. × 57,000.

Fig. 6. Martensitic growth of nitride plates into thick areas of a tantalum specimen. The transformation occurred in 35 torr of nitrogen at 300°C and caused sharp movement of the specimen. For the purpose of photographic recording the transformation was suppressed, by lowering the specimen temperature to 260°C. Operating voltage 1 MV. × 29,000.

Fig. 7. A similar specimen to that shown in Fig. 6, but photographed after a fully martensitic structure has formed. Operating voltage 1 MV. × 25,000.

Fig. 8. An unreacted spot in a pre-examined region of a nitrided tantalum specimen. It is believed that carbon contamination deposited during the pre-reaction period protects the tantalum from the reacting gas. Operating voltage 1 MV. × 8000.

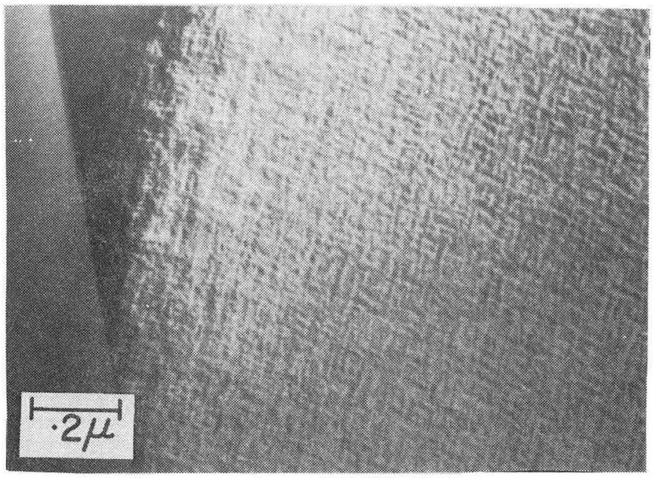

Figure 2

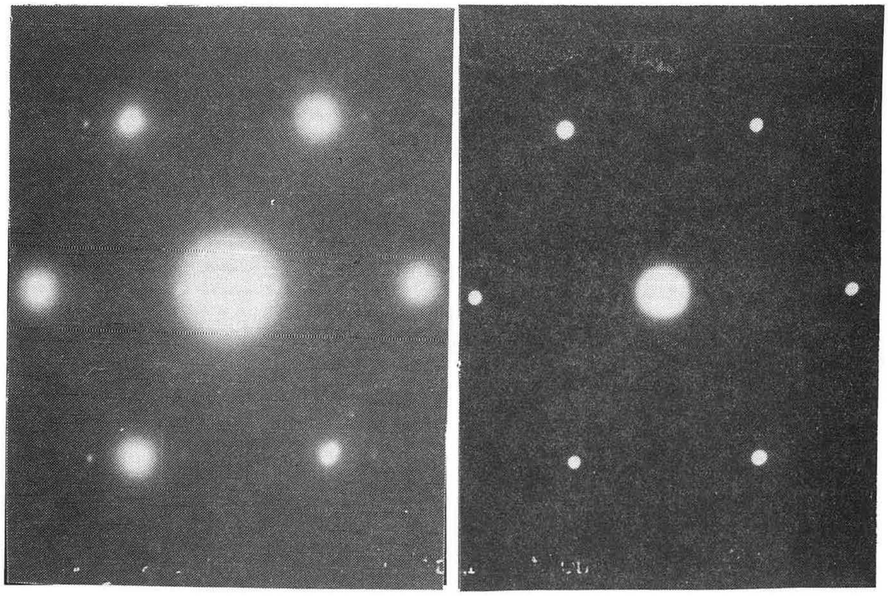
(a) (b)

XBB 732-1472

Figure 3

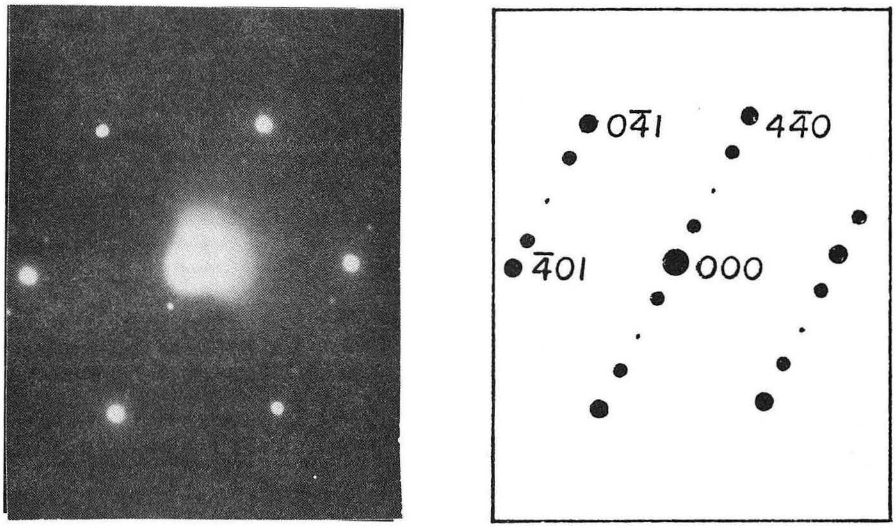

(a) (b)

Figure 4

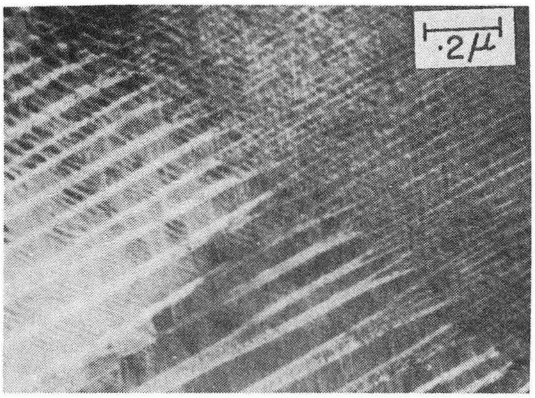

Figure 5

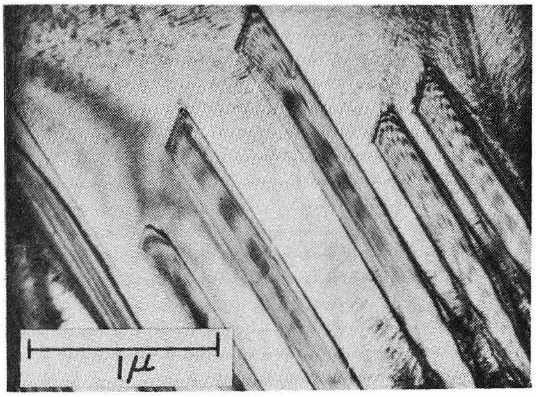

Figure 6

Figure 7

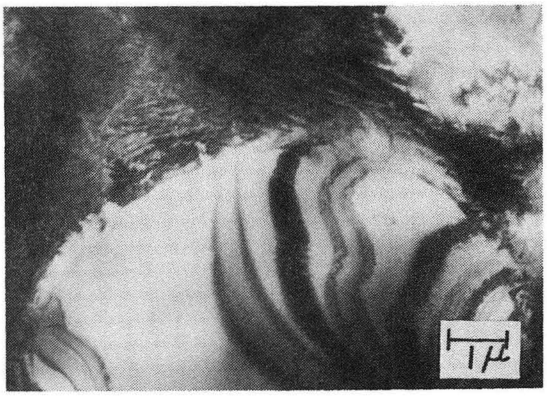

XBB 732-1471

Figure 8

TECHNICAL INFORMATION DIVISION
LAWRENCE BERKELEY LABORATORY
UNIVERSITY OF CALIFORNIA
BERKELEY, CALIFORNIA 94720